

工學碩士 學位論文

A Study on Viscous Damping Effects
in Leaf Spring Damper

指導教授 金 鍾 壽

2000年 2月

韓國海洋大學校 大學院

機械工學科

/

Abstract.....	1
1.	3
1.1	3
1.2	4
2.	5
2.1	5
2.2	9
2.2.1	9
2.2.2 O-	12
3.	15
4.	18
4.1	18
4.2	19
5.	24
5.1	24
5.2	26
6.	28
.....	29

/

- Fig.2.1 A sectional view of Leaf Spring Damper
- Fig.2.2 A free body diagram for a Leaf Spring Damper pack
- Fig.2.3 Detail of clamping structure of Leaf Spring pack
- Fig.2.4 Coordinates system of Leaf Spring Damper
- Fig.2.5 Schematic diagram for volumetric change of oil cabin by moving inner ring
- Fig.4.1 A prototype Leaf Spring Damper
- Fig.4.2 Photography of Leaf Spring Damper (Type C)
- Fig.4.3 A same model of CNC machine for application of LSD
- Fig.4.4 Attachment configuration of LSD to CNC machine
- Fig.4.5 Schematic diagram of test rig
- Fig.4.6 Photography of experiment system
- Fig.5.1 Illustration of displacements and reaction forces
(Type A,500rpm)
- Fig.5.2 Illustration of displacements and reaction forces
(Type B,500rpm)
- Fig.5.3 Hysteresis loops of LSD (without oil,500rpm)
- Fig.5.4 Hysteresis loops of LSD (without oil,3000rpm)
- Fig.5.5 Hysteresis loops of LSD (Type A, 500rpm)
- Fig.5.6 Hysteresis loops of LSD (Type A, 3000rpm)
- Fig.5.7 Hysteresis loops of LSD (Type B, 500rpm)
- Fig.5.8 Hysteresis loops of LSD (Type B, 3000rpm)
- Fig.5.9 Stiffness coefficients of prototype LSD
- Fig.5.10 Damping coefficients of prototype LSD

- Fig.5.11 Hysteresis loops of LSD (without oil,1000rpm,x-direction)
- Fig.5.12 Hysteresis loops of LSD (100cst,1000rpm,x-direction)
- Fig.5.13 Hysteresis loops of LSD (1000cst,1000rpm,x-direction)
- Fig.5.14 Hysteresis loops of LSD (3000cst,1000rpm,x-direction)
- Fig.5.15 Hysteresis loops of LSD (without oil,1000rpm,y-direction)
- Fig.5.16 Hysteresis loops of LSD (100cst,1000rpm,y-direction)
- Fig.5.17 Hysteresis loops of LSD (1000cst,1000rpm,y-direction)
- Fig.5.18 Hysteresis loops of LSD (3000cst,1000rpm,y-direction)
- Fig.5.19 Hysteresis loops of LSD (without oil,2000rpm,x-direction)
- Fig.5.20 Hysteresis loops of LSD (100cst,2000rpm,x-direction)
- Fig.5.21 Hysteresis loops of LSD (1000cst,2000rpm,x-direction)
- Fig.5.22 Hysteresis loops of LSD (3000cst,2000rpm,x-direction)
- Fig.5.23 Hysteresis loops of LSD (without oil,2000rpm,y-direction)
- Fig.5.24 Hysteresis loops of LSD (100cst,2000rpm,y-direction)
- Fig.5.25 Hysteresis loops of LSD (1000cst,2000rpm,y-direction)
- Fig.5.26 Hysteresis loops of LSD (3000cst,2000rpm,y-direction)
- Fig.5.27 Stiffness coefficients of prototype LSD (Type C)
- Fig.5.28 Damping coefficients of prototype LSD (Type C)

Table 4.1 Specification of prototype LSD

Table 4.2 Specification of test rig instruments

A	:	O	[mm]
b_o, h_o	:		[mm]
b	:		[mm]
$[C]$:		
C_{DR}, C_{DL}	:		
C_f	:	가	
$C_{xx}, C_{xy}, C_{yx}, C_{yy}$:		
d_o	:		[m]
E	:	, Young	[N/m ² , Pa]
F_N	:	O	[N]
F_s	:		[N]
$\Delta F_x, \Delta F_y$:		가 [N]
i	:		
I	:	2	[m ⁴]
$[K]$:		
K_s	:		
$K_{xx}, K_{xy}, K_{yx}, K_{yy}$:		
L_h	:		[m]
$M(x)$:		[N · m]
n	:		
p_i	:	i	[N/m ²]
P_i	:		[N]
ΔS_i	:		[mm]
t_i	:	i	[mm]

$(\Delta V)_i$:	i	[m3]
ΔV_f	:		[m3]
$\Delta x, \Delta y$:		[mm]
μ	:		
μ_o	:		
δ_i	:		[mm]
δ_{pre}	:		[mm]
ν	:	(Poisson's ratio)	
ϕ_i	:	i	[°]
η	:	[N · s/m2]	
ω	:	[rad/sec]	

A Study on Viscous Damping Effects in Leaf Spring Damper

Kim, Sang-Do

directed by Prof. Kim, Jong-Soo

Department of Mechanical Engineering
Graduate School, Korea Maritime University

Abstract

Recently, a new lateral vibration damper using leaf springs and oil, named as a leaf spring damper (LSD), developed by Jei and Kim.[2] The major advantage of this novel damper is that the dynamic characteristics of the leaf spring damper can be easily controlled by the design of side clearance and leaf spring packs. Therefore, the leaf spring dampers can be useful for turbomachinery, high speed spindles, vehicle axles, etc. In addition, since the leaf spring damper can directly cooperate with rolling element bearings, it ultimately extends the usage of rolling element bearings by providing damping property.

The present paper have been investigated experimentally the dynamic characteristics of a lateral leaf spring damper with different side clearance and oil viscosity. Experiments were performed to investigated the effects of side clearance and oil viscosity on the damping of lateral leaf spring damper. The stiffness and damping coefficients are obtained from the

displacements and the reaction forces generated by rotating the eccentric shaft. All dynamic coefficients are plotted with the excitation frequency which is adjusted by rotating speed of shaft. The test rig and two different leaf spring damper were manufactured to test the dynamic characteristics of the leaf spring damper.

가

가 .

, 가

가 ,

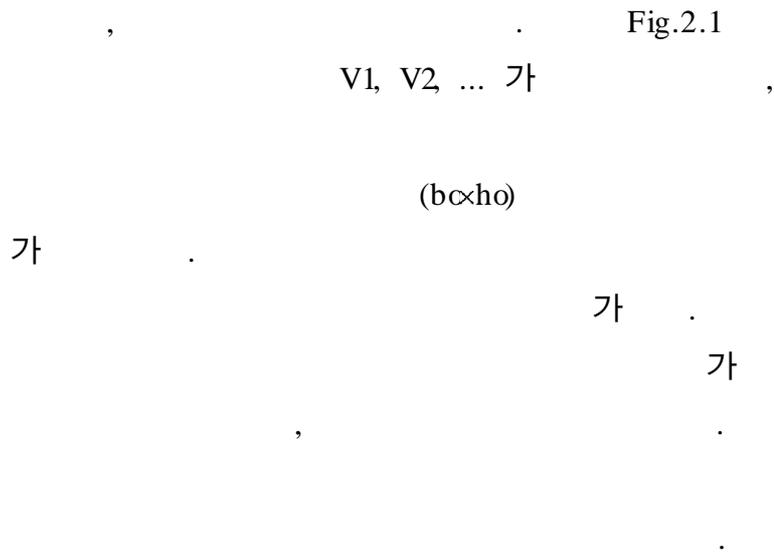
1.2

가

가

2.

Fig.2.1



2.1

Fig.2.2

$$(Pi) \quad (Mi) \quad (2.1) \quad .[9,10]$$

[

$$M_1(x) = - P_1(L_1 - x) + P_2(L_2 - x) + P_2 \langle x - L_2 \rangle^1 + \mu P_2(t_1/2 + \delta_2) - \mu P_2(t_1/2 + \delta_2) \langle x - L_2 \rangle^0 - \mu P_2 \delta_1(x) + \mu P_2 \delta_1(x) \langle x - L_2 \rangle^0$$

$$0 \leq x \leq L_i, \quad i = 1, 2, \dots, n-1 \quad (2.4)$$

$$\delta_n(x) = \frac{P_n}{6(EI)_n} (3L_n x^2 - x^3) \quad (2.5)$$

(2.4)

(2.5)

(2.6)

$$\begin{aligned} \frac{P_{i-1}}{6(EI)_{i-1}} (3L_{i-1}L_i^2 - L_i^3) - \frac{P_i L_i^3}{3(EI)_{i-1}} \\ = \frac{P_i L_i^3}{3(EI)_i} - \frac{P_{i+1}}{6(EI)_i} (3L_i L_{i+1}^2 - L_{i+1}^3) \end{aligned} \quad (2.6)$$

(2.6)

(2.7)

$$\begin{bmatrix} d_2 & c_2 & 0 & 0 & 0 & \dots & 0 \\ a_3 & d_3 & c_3 & 0 & 0 & \dots & 0 \\ 0 & a_4 & d_4 & c_4 & 0 & \dots & 0 \\ 0 & 0 & a_4 & d_5 & c_5 & \dots & 0 \\ \dots & \dots & \dots & \dots & \dots & \dots & \dots \\ 0 & 0 & 0 & \dots & a_{n-1} & d_{n-1} & c_{n-1} \\ 0 & 0 & 0 & \dots & 0 & a_n & d_n \end{bmatrix} \begin{pmatrix} \varphi_2 \\ \varphi_3 \\ \varphi_4 \\ \vdots \\ \varphi_{n-1} \\ \varphi_n \end{pmatrix} = \begin{pmatrix} b_2 \\ b_3 \\ b_4 \\ \vdots \\ b_{n-1} \\ b_n \end{pmatrix} \quad (2.7)$$

$$a_i = (3L_{i-1} - L_i)L_i^2/L_i^3$$

$$b_i = \begin{cases} -a_i & i = 2 \\ 0 & i = 3, 4, \dots, n \end{cases}$$

$$c_i = \frac{(EI)_{i-1}}{(EI)_i} a_{i+1}$$

$$d_i = -2 \left(\frac{L_i}{L_1} \right)^3 \left(1 + \frac{(EI)_{i-1}}{(EI)_i} \right)$$

$$\varphi_i = \frac{P_i}{P_1}$$

(2.8)

$$k_p = \frac{3(EI)_1}{\xi(1-\nu^2)L_1^3} \tag{2.8}$$

$$\xi = 1 - 0.5\varphi_2 \left(\frac{L_2}{L_1} \right)^2 \left\{ 3 - \left(\frac{L_2}{L_1} \right) \right\} \tag{2.9}$$

ν : (Poisson's ratio)

Fig.2.3

(2.10)

[11]

$$k_s = \frac{k_p}{(1 + a/L_1)} \tag{2.10}$$

a Fig.2.3

$a = l_1$

$a = l_2$

2.2

가

)

)

)

O-

가

2.2.1

Fig.2.4

$\Delta x, \Delta y$

Fig.2.5

i

$(\Delta V)_i$

$$(\Delta V)_i = (\Delta V_s)_i + (\Delta V_f)_i - (\Delta V_f)_{i+1} \quad (2.11)$$

ΔV_s

$$(\Delta V_s)_i = \frac{bd_o}{2} \{ (\sin \phi_{i+1} - \sin \phi_i) \Delta x + (\cos \phi_i - \cos \phi_{i+1}) \Delta y \} \quad (2.12)$$

d_o , b
 ϕ_i x i
 ΔV_f
 k_s (cantilever
 beam) δ_1
 $\delta(x)$ (2.13)

$$\delta(x) = \frac{1}{2L^3}(3Lx^2 - x^3)\delta_1 \quad (2.13)$$

$$\Delta x, \Delta y \quad (2.14)$$

$$(\Delta V_f)_i = \frac{3bL}{8}(\cos \phi_i \Delta x + \sin \phi_i \Delta y) \quad (2.14)$$

$$(\Delta V_f)_{i+1} = \frac{3bL}{8}(\cos \phi_{i+1} \Delta x + \sin \phi_{i+1} \Delta y)$$

가

L

$$\begin{aligned}
 (\Delta V)_i = & \left\{ \frac{bd_o}{2}(\sin \phi_{i+1} - \sin \phi_i) + \frac{3bL}{8}(\cos \phi_i - \cos \phi_{i+1}) \right\} \Delta x \\
 & + \left\{ \frac{bd_o}{2}(\cos \phi_i - \cos \phi_{i+1}) + \frac{3bL}{8}(\sin \phi_i - \sin \phi_{i+1}) \right\} \Delta y
 \end{aligned} \quad (2.15)$$

(oil groove) 가 가
 가 . 가
 (2.16) .

$$(Q_s)_i = C_{DR}(p_i - p_{i-1}) + C_{DL}(p_i - p_{i+1}) \tag{2.16}$$

C_{DR}, C_{DL} 가
 (2.17) 가 .[13]

$$C_D = 2 \left(\frac{\pi d_h^4}{142 \eta L_h} \right), \quad d_h = \frac{2b_o h_o}{b_o + h_o} \tag{2.17}$$

b_o, h_o , L_h
 . η
 가

2 . 가

$$(2.18) ,$$

$$(Q_s)_i = \frac{d(\Delta V)_i}{dt} \tag{2.18}$$

(2.15),(2.16) (2.18)
 (2.19) .

$$\begin{aligned}
p_{i-1} - 2p_i + p_{i+1} = & \frac{3bL}{8C_D} \left\{ -\frac{4d_o}{3L} (\sin \phi_i - \sin \phi_{i+1}) + (\cos \phi_i - \cos \phi_{i+1}) \right\} \frac{d(\Delta x)}{dt} \\
& + \frac{3bL}{8C_D} \left\{ \frac{4d_o}{3L} (\cos \phi_i - \cos \phi_{i+1}) + (\sin \phi_i - \sin \phi_{i+1}) \right\} \frac{d(\Delta y)}{dt}
\end{aligned}
\tag{2.19}$$

$$p_i = \dots
\tag{2.20}$$

$$P = P_0 + \Delta P$$

$$\Delta p = \left(\frac{\partial p}{\partial \dot{x}} \right) \frac{d(\Delta x)}{dt} + \left(\frac{\partial p}{\partial \dot{y}} \right) \frac{d(\Delta y)}{dt} = p_x \cdot \Delta \dot{x} + p_y \cdot \Delta \dot{y}
\tag{2.20}$$

$$(2.19) \quad x- \quad y-
\tag{2.20}$$

2.2.2 O-

$$O- \quad 1 \quad E$$

$$E = 4\mu_o F_N A
\tag{2.21}$$

$$FN \quad O- \quad , A \quad , \mu_o$$

가 C_f

$$C_f = \frac{4\mu_o F_N}{\pi\omega A} \quad (2.22)$$

(hysteresis damping)

F_s

$$F_s = k_s \delta + j h_d \dot{\delta} = k_s (1 + j \zeta) \delta \quad (2.23)$$

$j h_d \dot{\delta}$

$\zeta = h_d / k_s$

$$C_h = \frac{h_d}{\omega} = \frac{\zeta k_s}{\omega} \quad (2.24)$$

ζ

(Dissipation energy, E_d)

$$E_d = 4 \mu_s P_1 \Delta s_1 + \sum_{i=2}^n 4 \mu_s P_i (2 \Delta s_i) \quad (2.25)$$

n

, Δs_i

Δs_i

$2 \Delta s_i$

$$\delta_i \quad (2.26)$$

$$\Delta s_i = \frac{3 \delta_i t_i}{2 L_i} \quad (2.26)$$

$$t_i \quad , \quad (2.25) \quad (2.27)$$

$$E_d = 6 \mu_s k_s (\delta_1 + \delta_{pre}) \delta_1 \left[\frac{t_1}{L_1} + 2 \sum_{i=2}^n \varphi_i \frac{\delta_i}{\delta_1} \frac{t_i}{L_i} \right] \quad (2.27)$$

$$(2.27) \quad \delta_{pre} \quad (\text{preload}) \quad .$$

$$\xi \quad (2.28) \quad .$$

$$\xi = \frac{6 \mu_s}{\pi} \left(1 + \frac{\delta_{pre}}{\delta_1} \right) \left[\frac{t_1}{L_1} + 2 \sum_{i=2}^n \varphi_i \frac{\delta_i}{\delta_1} \frac{t_i}{L_i} \right] \quad (2.28)$$

3.

Fig.2.4

(3.1)

$$F_i = k_s(1 + j\eta) \cos \phi_i \Delta x + k_s(1 + j\eta) \sin \phi_i \Delta y + \frac{3bL}{8}(p_{i-1} - p_i) \quad (3.1)$$

(3.1)

(3.2) (3.3)

[15]

$$\begin{aligned} F_x &= \sum_{i=1}^N \left\{ F_i \cos \phi_i + \frac{bd_o}{2} \int_{\phi_i}^{\phi_{i+1}} p_i \cos \theta d\theta \right\} \\ &= K_{xx} \Delta x + K_{xy} \Delta y + C_{xx} \Delta \dot{x} + C_{xy} \Delta \dot{y} \end{aligned} \quad (3.2)$$

$$\begin{aligned} F_y &= \sum_{i=1}^N \left\{ F_i \sin \phi_i + \frac{bd_o}{2} \int_{\phi_i}^{\phi_{i+1}} p_i \sin \theta d\theta \right\} \\ &= K_{yx} \Delta x + K_{yy} \Delta y + C_{yx} \Delta \dot{x} + C_{yy} \Delta \dot{y} \end{aligned} \quad (3.3)$$

(3.2)

(3.3)

(3.2), (3.3)

(3.1)

(3.4)

(3.5)

:

$$\begin{aligned}
K_{xx} &= k_s \sum_{i=1}^N \cos^2 \phi_i \\
K_{xy} &= k_s \sum_{i=1}^N \sin \phi_i \cos \phi_i \\
K_{yx} &= k_s \sum_{i=1}^N \cos \phi_i \sin \phi_i \\
K_{yy} &= k_s \sum_{i=1}^N \sin^2 \phi_i
\end{aligned} \tag{3.4}$$

:

$$\begin{aligned}
C_{yy} &= C_f + \frac{\xi k_s}{\omega} \sum_{i=1}^N \sin^2 \phi_i \\
&\quad + \lambda \sum_{i=1}^N \left\{ \left(\bar{p}_{x,i-1} - \bar{p}_{y,i} \right) \sin \phi_i - \frac{4d_o}{3L} \bar{p}_{y,i} \left(\cos \phi_i - \cos \phi_{i+1} \right) \right\} \\
C_{xx} &= C_f + \frac{\xi k_s}{\omega} \sum_{i=1}^N \cos^2 \phi_i \\
&\quad + \lambda \sum_{i=1}^N \left\{ \left(\bar{p}_{x,i-1} - \bar{p}_{x,i} \right) \cos \phi_i + \frac{4d_o}{3L} \bar{p}_{x,i} \left(\sin \phi_i - \sin \phi_{i+1} \right) \right\} \\
C_{xy} &= \frac{\xi k_s}{\omega} \sum_{i=1}^N \sin \phi_i \cos \phi_i \\
&\quad + \lambda \sum_{i=1}^N \left\{ \left(\bar{p}_{y,i-1} - \bar{p}_{y,i} \right) \cos \phi_i + \frac{4d_o}{3L} \bar{p}_{y,i} \left(\sin \phi_i - \sin \phi_{i+1} \right) \right\} \\
C_{yx} &= \frac{\xi k_s}{\omega} \sum_{i=1}^N \cos \phi_i \sin \phi_i \\
&\quad + \lambda \sum_{i=1}^N \left\{ \left(\bar{p}_{x,i-1} - \bar{p}_{x,i} \right) \sin \phi_i - \frac{4d_o}{3L} \bar{p}_{x,i} \left(\cos \phi_i - \cos \phi_{i+1} \right) \right\}
\end{aligned} \tag{3.5}$$

$$\lambda \tag{3.6}$$

$$\lambda = \frac{9b^2L^2}{64C_D} = \frac{639\eta L_h b^2 L^2}{64\pi d_h^4} \quad (3.6)$$

$$\bar{P}_x, \bar{P}_y = \frac{8C_D}{3bL} P_x, P_y$$

k_s 가

$$(3.4) \quad K_{xy} = K_{yx} = 0$$

$$K_{xx} = K_{yy} = 0.5Nk_s \quad (\text{isotropic})$$

O-

가

4.

4.1

Fig. 2.1 Fig. 4.1

,
CNC

Fig. 4.2

. Fig. 4.3

. CNC

가

, Fig. 4.4

가

. Fig. 4.1

#6911

6

가

가

(Type A :

0.25mm, Type B : 0.10mm)

Table 4.1

Fig.

4.5

가

50 μ m

가

,

가

(eddy current type displacement trasducer)

(load cell)

(Amplifier)

A/D

가

Table 4.2

가

가

(cross couple term)

가

[2]

가 .

Fig.

4.6 .

4.2

가 , Fourier

. [8]

(4.1)

가 . [7,8]

$$\begin{Bmatrix} \Delta F_x \\ \Delta F_y \end{Bmatrix} = [K] \begin{Bmatrix} \Delta x \\ \Delta y \end{Bmatrix} + [C] \begin{Bmatrix} \dot{\Delta x} \\ \dot{\Delta y} \end{Bmatrix} + [m] \begin{Bmatrix} \ddot{\Delta x} \\ \ddot{\Delta y} \end{Bmatrix} \quad (4.1)$$

[K] [C]

가 (4.2)

$$\Delta F_x = A \sin(\omega_x t - \alpha_1) \quad (4.2)$$

$$\Delta F_y = B \sin(\omega_y t - \alpha_2)$$

(4.3)

$$\Delta x = a_1 \cos \omega_x t + a_2 \sin \omega_x t + a_3 \cos \omega_y t + a_4 \sin \omega_y t \quad (4.3)$$

$$\Delta y = b_1 \cos \omega_x t + b_2 \sin \omega_x t + b_1 \cos \omega_y t + b_2 \sin \omega_y t$$

가

가

$$\omega_x = \omega_y = \omega \quad (4.3) \quad (4.1)$$

(4.4),(4.5) .

$$\begin{aligned} \Delta F_x &= [m](-a_1\omega^2 \cos \omega t - a_2\omega^2 \sin \omega t) + [C](-a_1\omega \sin \omega t + a_2\omega \cos \omega t) \\ &\quad + [K](a_1 \cos \omega t + a_2 \sin \omega t) \\ &= (-a_1\omega^2[m] + a_2\omega[C] + a_1[K]) \cos \omega t \\ &\quad + (-a_2\omega^2[m] - a_1\omega[C] + a_2[K]) \sin \omega t \end{aligned} \quad (4.4)$$

$$\begin{aligned} \Delta F_y &= [m](-b_1\omega^2 \cos \omega t - b_2\omega^2 \sin \omega t) + [C](-b_1\omega \sin \omega t + b_2\omega \cos \omega t) \\ &\quad + [K](b_1 \cos \omega t + b_2 \sin \omega t) \\ &= (-b_1\omega^2[m] + b_2\omega[C] + b_1[K]) \cos \omega t \\ &\quad + (-b_2\omega^2[m] - b_1\omega[C] + b_2[K]) \sin \omega t \end{aligned} \quad (4.5)$$

$$(4.3) \quad \cos \omega t, \sin \omega t \quad t$$

(4.6),(4.7)

a_1, a_2, b_1, b_2 가 .

$$\begin{aligned} \int_0^\tau \cos \omega t \cdot \Delta x \, dt &= a_1 \int_0^\tau \cos^2 \omega t \, dt + a_1 \int_0^\tau \cos \omega t \sin \omega t \, dt \\ &= a_1 \int_0^\tau \cos^2 \omega t \, dt = \frac{\tau}{2} \cdot a_1 \end{aligned}$$

$$\begin{aligned} a_1 &= \frac{2}{\tau} \int_0^\tau \Delta x \cos \omega t \, dt \\ a_2 &= \frac{2}{\tau} \int_0^\tau \Delta x \sin \omega t \, dt \end{aligned} \quad (4.6)$$

$$b_1 = \frac{2}{\tau} \int_0^{\tau} \Delta y \cos \omega t \, dt \quad (4.7)$$

$$b_2 = \frac{2}{\tau} \int_0^{\tau} \Delta y \sin \omega t \, dt$$

{a}, {b}

$$\{a\} = \begin{Bmatrix} a_1 \\ a_2 \end{Bmatrix} = \frac{2}{\tau} \begin{Bmatrix} \int_0^{\tau} \Delta x \cos \omega t \, dt \\ \int_0^{\tau} \Delta x \sin \omega t \, dt \end{Bmatrix} \quad (4.6a)$$

$$\{b\} = \begin{Bmatrix} b_1 \\ b_2 \end{Bmatrix} = \frac{2}{\tau} \begin{Bmatrix} \int_0^{\tau} \Delta y \cos \omega t \, dt \\ \int_0^{\tau} \Delta y \sin \omega t \, dt \end{Bmatrix} \quad (4.7a)$$

(4.3)

(4.6),(4.7)

(4.4),(4.5)

(4.8),(4.9),(4.10)(4.11)

$$\begin{aligned} \int_0^{\tau} \Delta F_x \cos \omega t \, dt = & (-a_1 \omega^2 [m] + a_2 \omega [C] + a_1 [K]) \int_0^{\tau} \cos^2 \omega t \, dt \\ & + (-a_2 \omega^2 [m] - a_1 \omega [c] + a_2 [K]) \int_0^{\tau} \cos \omega t \sin \omega t \, dt \end{aligned}$$

$$-a_1 \omega^2 [m] + a_2 \omega [C] + a_2 [K] = \frac{2}{\tau} \int_0^{\tau} \Delta F_x \cos \omega t \, dt \quad (4.8)$$

$$-a_2 \omega^2 [m] - a_1 \omega [c] + a_2 [K] = \frac{2}{\tau} \int_0^{\tau} \Delta F_x \sin \omega t \, dt \quad (4.9)$$

$$-b_1 \omega^2 [m] - b_2 \omega [C] + b_1 [K] = \frac{2}{\tau} \int_0^{\tau} \Delta F_y \cos \omega t \, dt \quad (4.10)$$

$$- b_2 \omega^2 [m] - b_1 \omega [C] + b_2 [K] = \frac{2}{\tau} \int_0^\tau \Delta F_y \sin \omega t dt \quad (4.11)$$

$$a_1, a_2, b_1, b_2, [m] \quad , \quad [C], [K]$$

$$(4.8), (4.9), (4.10), (4.11)$$

$$[C], [K] \quad .$$

$$\begin{bmatrix} K_{xx} \\ C_{xx} \end{bmatrix} = [U]^{-1} [u_1] \quad , \quad \begin{bmatrix} K_{yy} \\ C_{yy} \end{bmatrix} = [U]^{-1} [u_2] \quad (4.12)$$

$$[U] = \begin{bmatrix} a_1 & b_1 & a_2 \omega & b_2 \omega \\ a_2 & b_2 & -a_1 \omega & -b_1 \omega \end{bmatrix} \quad (4.13)$$

$$\{u_1\} = \{c\} + m \{e\} \quad (4.14)$$

$$\{u_2\} = \{d\} + m \{f\}$$

$$\{c\}, \{d\} \quad \{e\}, \{f\} \quad (4.15), (4.16), (4.17), (4.18) \quad .$$

$$\{c\} = \begin{Bmatrix} c_1 \\ c_2 \end{Bmatrix} = \frac{2}{\tau} \begin{Bmatrix} \int_0^\tau \Delta F_x \cos \omega t dt, \\ \int_0^\tau \Delta F_x \sin \omega t dt \end{Bmatrix} \quad (4.15)$$

$$\{d\} = \begin{Bmatrix} d_1 \\ d_2 \end{Bmatrix} = \frac{2}{\tau} \begin{Bmatrix} \int_0^\tau \Delta F_y \cos \omega t dt, \\ \int_0^\tau \Delta F_y \sin \omega t dt \end{Bmatrix} \quad (4.16)$$

$$\{e\} = \begin{Bmatrix} e_1 \\ e_2 \end{Bmatrix} = \begin{Bmatrix} a_1 \omega^2 \\ a_2 \omega^2 \end{Bmatrix} \quad (4.17)$$

$$\{f\} = \begin{Bmatrix} f_1 \\ f_2 \end{Bmatrix} = \begin{Bmatrix} b_1 \omega^2 \\ b_2 \omega^2 \end{Bmatrix} \quad (4.18)$$

(4.6a),(4.7a),(4.15),(4.16),(4.17),(4.18) $\{a\}, \{b\}, \{c\}, \{d\}, \{e\}, \{f\}$

fourier

$\{a\}, \{b\}, \{e\}, \{f\}$, $\{c\}, \{d\}$ Load cell

FFT

(4.19),(4.20),(4.21),(4.22)

$$K_{xx} = \frac{1}{(a_1^2 - a_2^2)\omega} [a_1 \omega (c_1 + a_1 \omega^2 m) - a_2 \omega (c_2 + a_2 m \omega)] \quad (4.19)$$

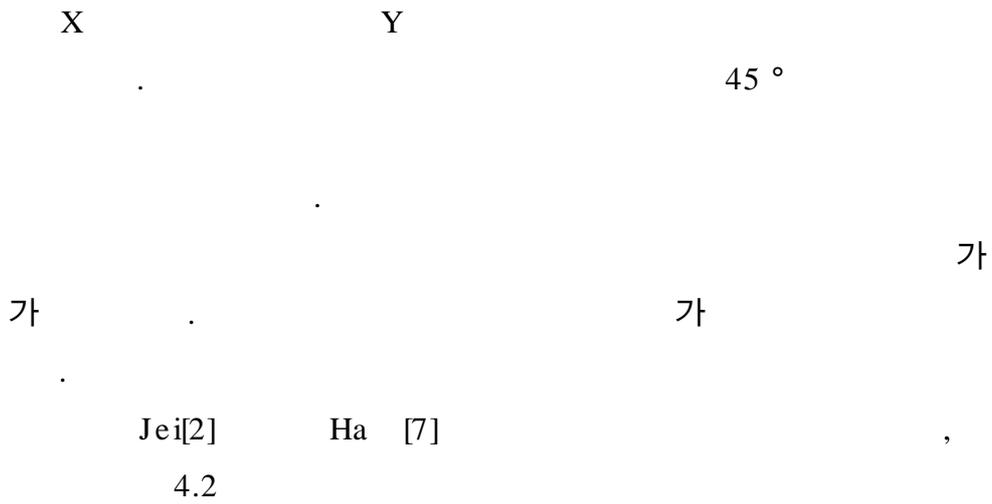
$$K_{yy} = \frac{1}{(b_1^2 - b_2^2)\omega} [b_1 \omega (d_1 + b_1 \omega^2 m) - b_2 \omega (d_2 + b_2 m \omega)] \quad (4.20)$$

$$C_{xx} = \frac{1}{(a_1^2 - a_2^2)\omega} [-a_2 (c_1 + a_1 m \omega^2) + a_1 \omega (c_2 + a_2 m \omega)] \quad (4.21)$$

$$C_{yy} = \frac{1}{(b_1^2 - b_2^2)\omega} [-b_2 (d_1 + b_1 m \omega^2) + b_1 \omega (d_2 + b_2 m \omega)] \quad (4.22)$$

5.

Fig. 2.4



5.1

Table 4.1		가		Type
A	Type B			Fig.
5.1	Fig. 5.2	200N	300N	50
μm		가	Type B가 Type A	
	가		가	
Type A	Type B			

(hysteresis loop)

Fig. 5.3

Fig. 5.8

가

가

가

가

(cavity)

가

가 500rpm

Fig.5.5 Fig.5.7 Type B

가 Type B 가

가 Fig.5.6 Fig.5.8

가 3000rpm Type B

가 가

가 가

가 가

Type A

Type B Fig.5.9

가

가

가

가

Fig.5.10 Type A Type B Type A

Type B 가 , 가 가

가 가

가 가 ,
 가
 가 가
 가
 가 가
 가
 가

5.2

Table 4.1 Type C 가

가 100cst, 1000cst, 3000cst 가

Fig. 5. 26

Fig. 5.11

Fig. 5.12 Fig. 5.13

100cst 1000cst

가
 가 가

Fig. 5.13 Fig.

5.17

가

Fig. 5.13 Fig.

5.21

1000rpm

2000rpm

가

가

Fig. 5.20

Fig. 5.21

가 100cst

1000cst

180N

280N

50%

가

가

Fig. 5.20

Fig. 5.24

가

Fig. 5.27

Fig. 5.28

Fig. 5.27

가

가

가

Fig. 5.28

가 100cst

1000cst

가

가

가

가

가

가

가

가

가

6.

1. 가 , 가
가 .
2. 가
3. 가 .
4. 가 가 ,
가 .
5. 가 .
6. 가 .
- 7.

- [1] , , , “
”;
, 1999
- [2] Jei, Y.-G., Kim, J.-S., Hong, S.-W., and Jung, S.-Y., "A New Lateral Vibration Damper Using Leaf Springs.", ASME Trans. J. of Vib. and Acoustics, Vol.121, No2, 1999
- [3] , , , “
”;
, 1999
- [4] , , , , “
”;
, 18 , 1 , 1994, pp11-22.
- [5] , , , , “
”;
, 18 , 1 , 1994, pp23-31.
- [6] Kostrewwsky, G. J. and Flack, R. D., "Accuracy Evaluation of Experimentally Derived Dynamic Coefficients of Fluid Film Bearings Part : Development of Method", STLE Trans., Vol.33, 1990, pp.105-114.
- [7] Ha, H.-C., and Yang, S. H., "Excitation Frequency Effects on the Stiffness and Damping Coefficients of a Five-Pad Tilting Pad Journal Bearing", ASME Trans., J. of Tribology, 98-TRIB-44.
- [8] , , , “가 가
”;
, 14 , 1 , 1998,
pp14-22
- [9] , “
”;
, 1997
- [10] Spatts, M.E., Design of Machine Elements, 6th edition, Prentice-Hall, 1985

- [11] Crandall, S. H., Dahl, N. C., and Lardner, T. J., "An Introduction to the Mechanics of Solids, 2nd edition, McGraw-Hill, 1978
- [12] Fung, Y. C., "Foundations of Solid Mechanics", Prentice-Hall, Toronto, 1965
- [13] Schlichting, H., "Boundary-Layer Theory", 7th edition, McGraw-Hill, 1965
- [14] , , , " " ; , 12 , 13 , 1995, pp175-181
- [15] James, M.L., Smith, G.M., Wolford, J.C., and Whaley, P.W., "Vibration of Mechanical and Structural Systems, Harper & Row,
- [16] Burrows, C.R. and Sahinkaya, M.N., "Frequency Domain Estimation of Linearized Oil Film Coefficients", J. of Tribology, Trans. of ASME, Vol. 104, 1982, pp 210-215
- [17] Nicholas, J.C., Gunter, E.J., and Allaire, P.E., "Effect of residual shaft bow on unbalance response and balancing of a single mass flexible rotor: part -Unbalance response," Trans. ASME, Journal of Engineering for Power, Vol 98, No. 2, 1976, pp171-181

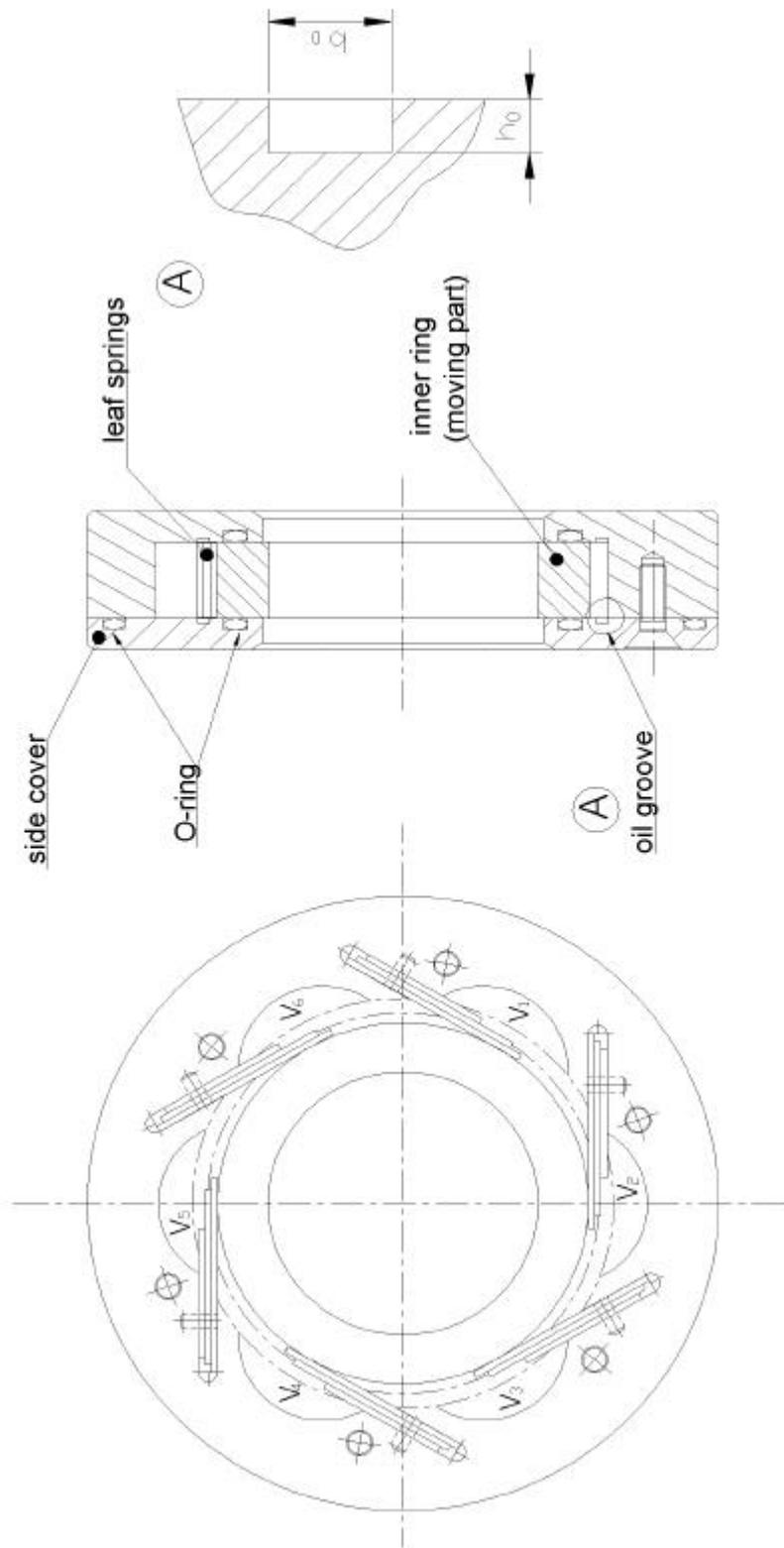


Fig.2.1 A sectional view of Leaf Spring Damper

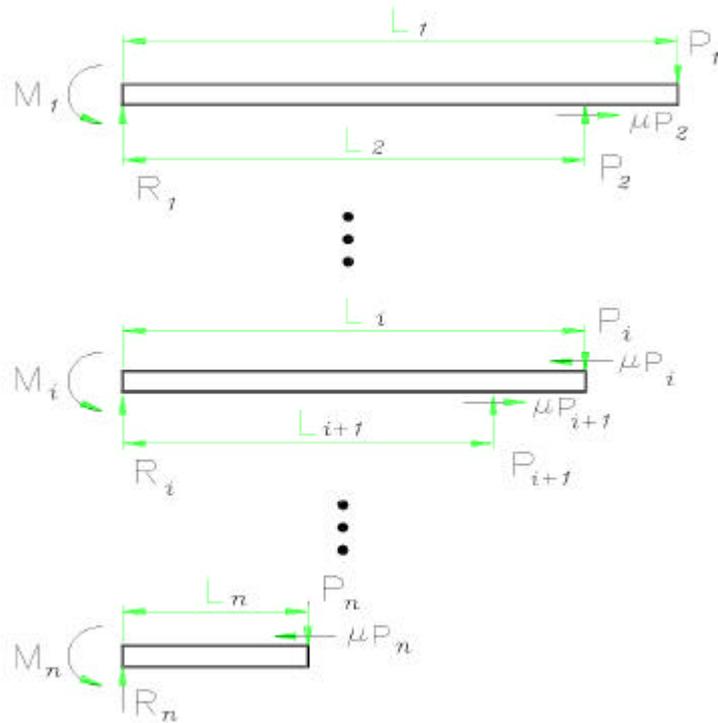


Fig.2.2 A free body diagram for a Leaf Spring Damper pack

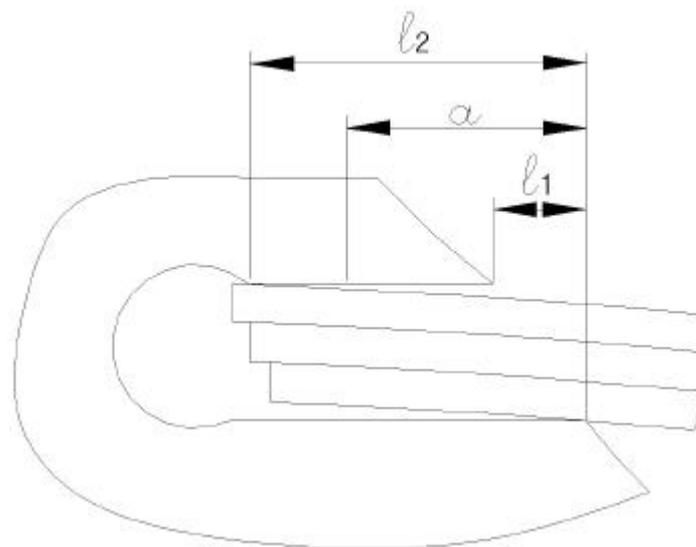


Fig.2.3 Detail of clamping structure of Leaf Spring pack

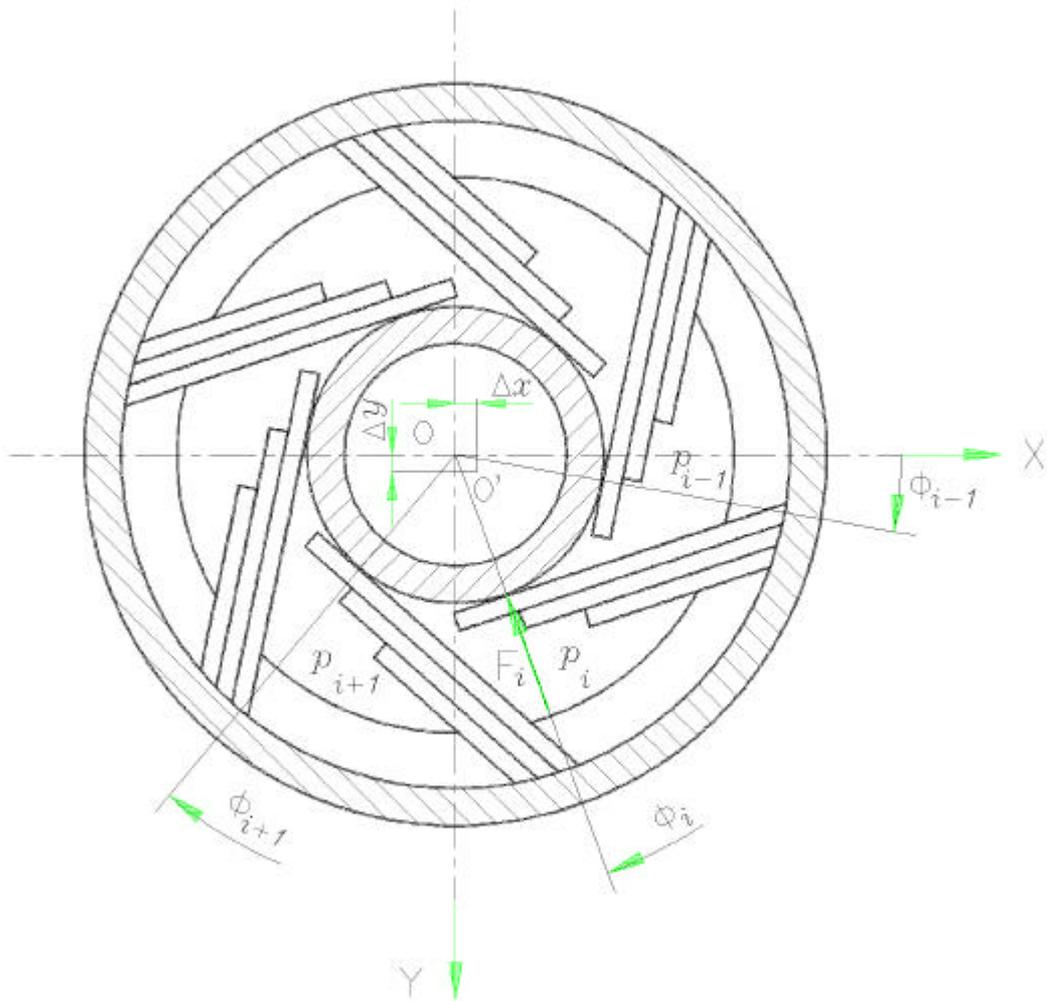


Fig.2.4 Coordinates system of Leaf Spring Damper

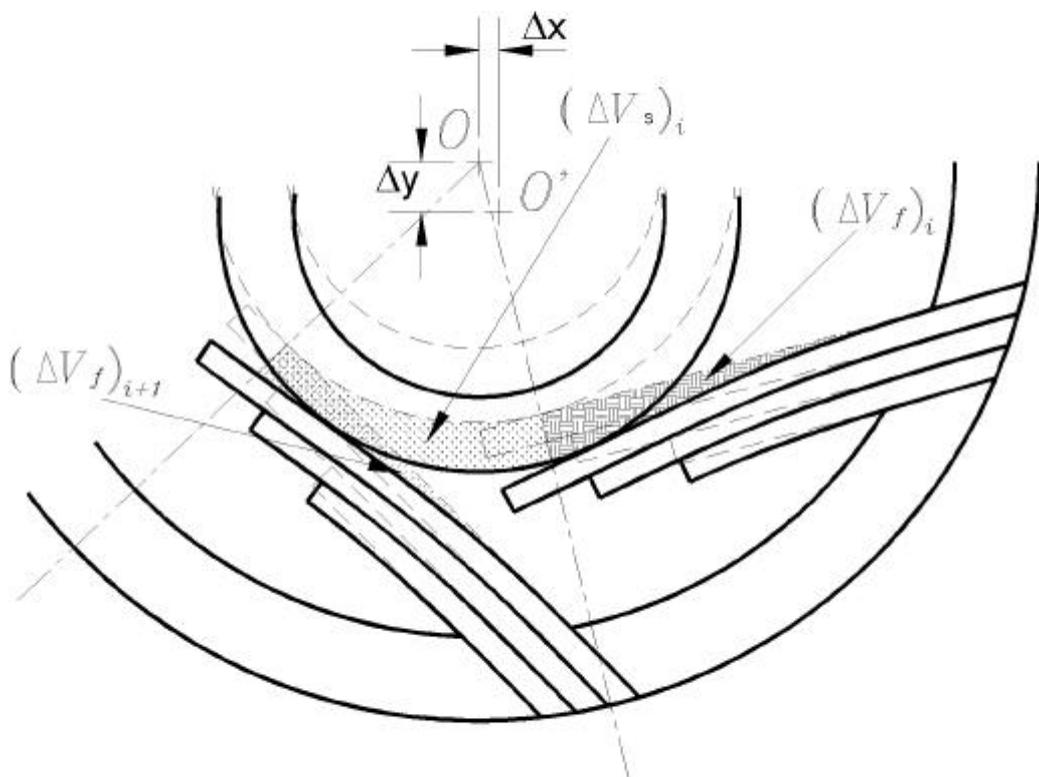


Fig.2.5 Schematic diagram for volumetric change of oil cabin by moving inner ring

Fgi.4.1 A prototype Leaf Spring Damper



Fig.4.2 Photography of Leaf Spring Damper (Type C)



Fig.4.3 A same model of CNC machine for application of LSD

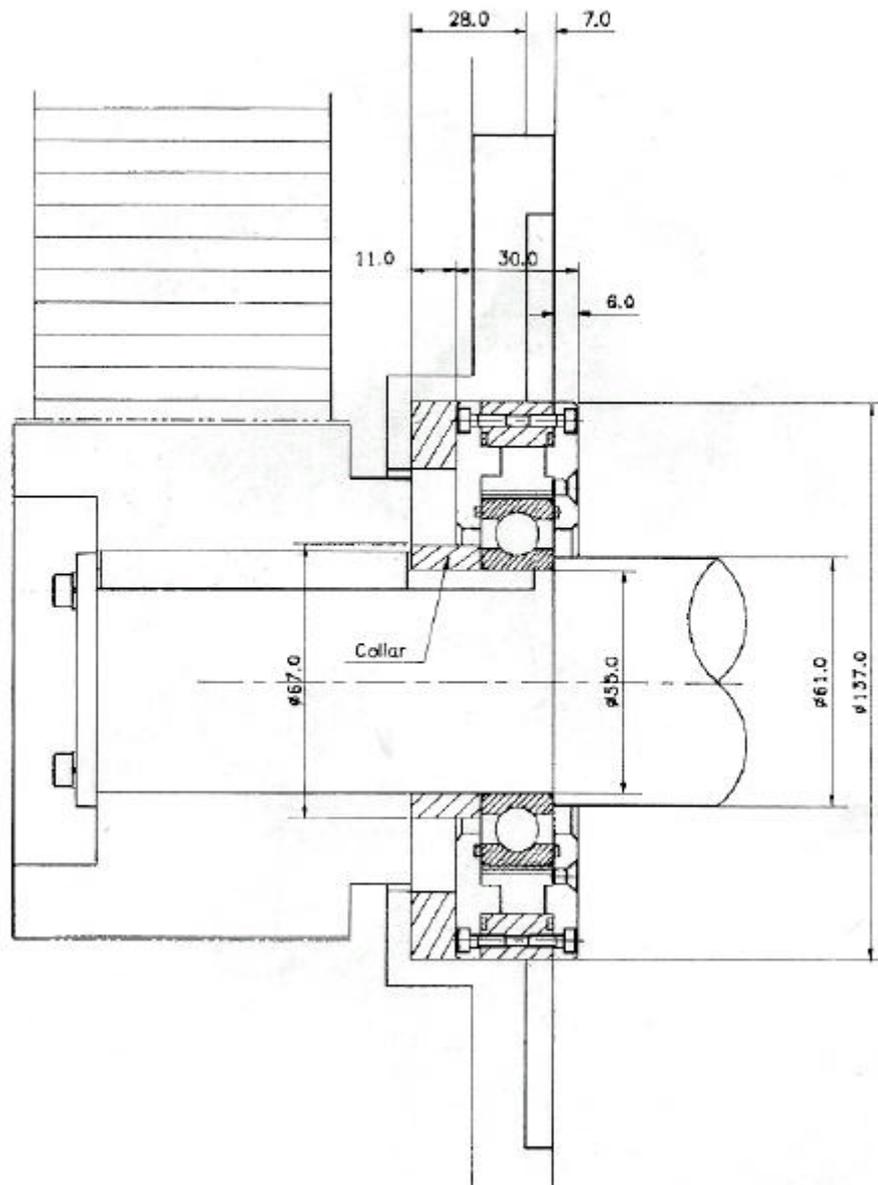


Fig.4.4 Attachment configuration of LSD to CNC machine

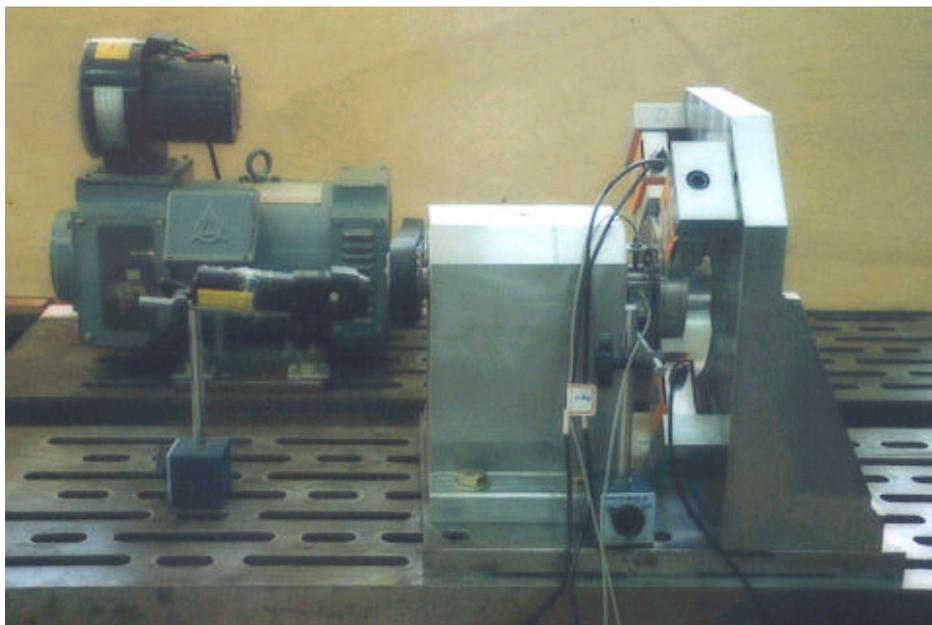
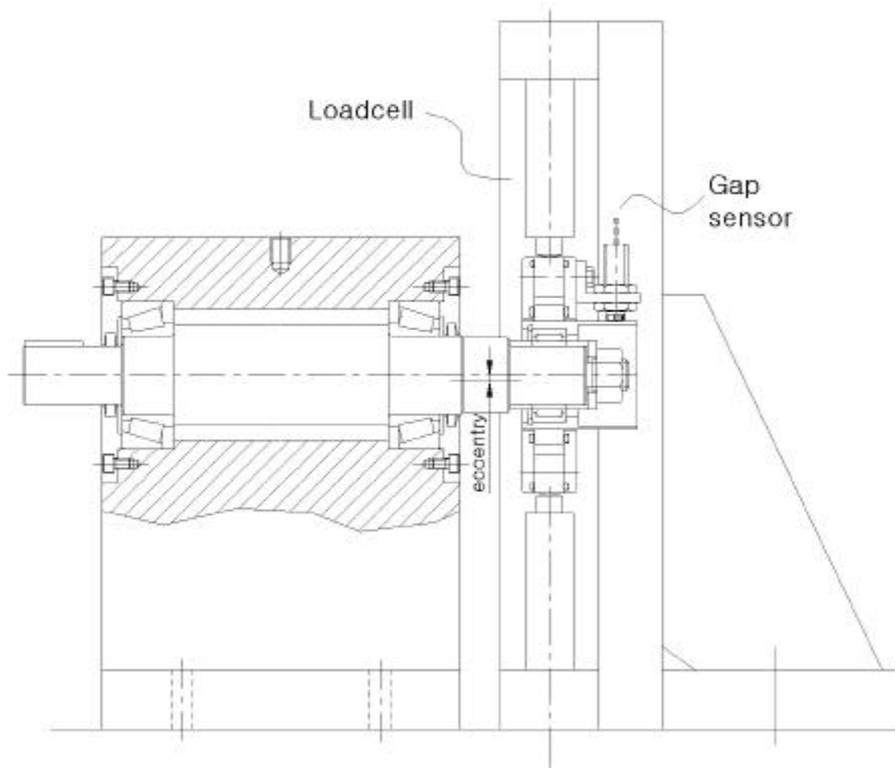


Fig.4.6 Photography of experiment system

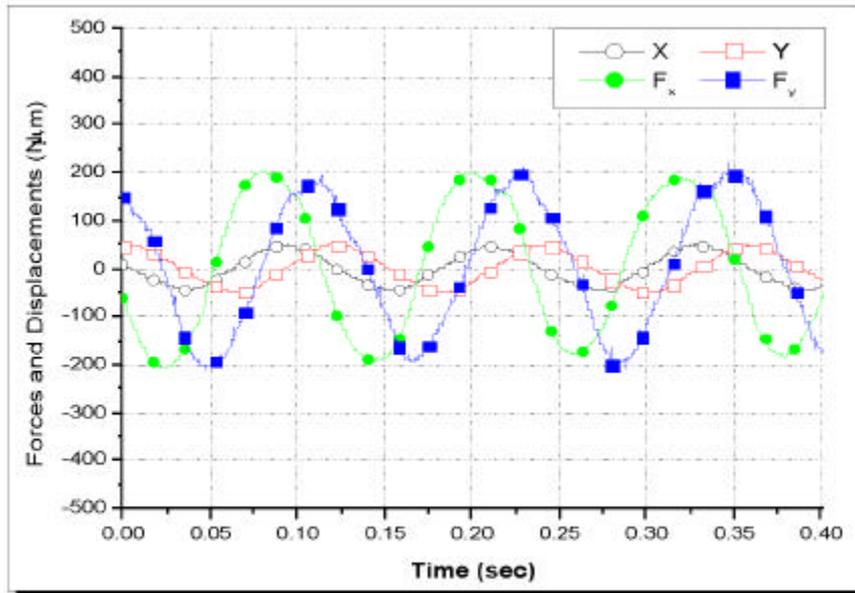


Fig.5.1 Illustration of displacements and reaction forces
(Type A, 500rpm)

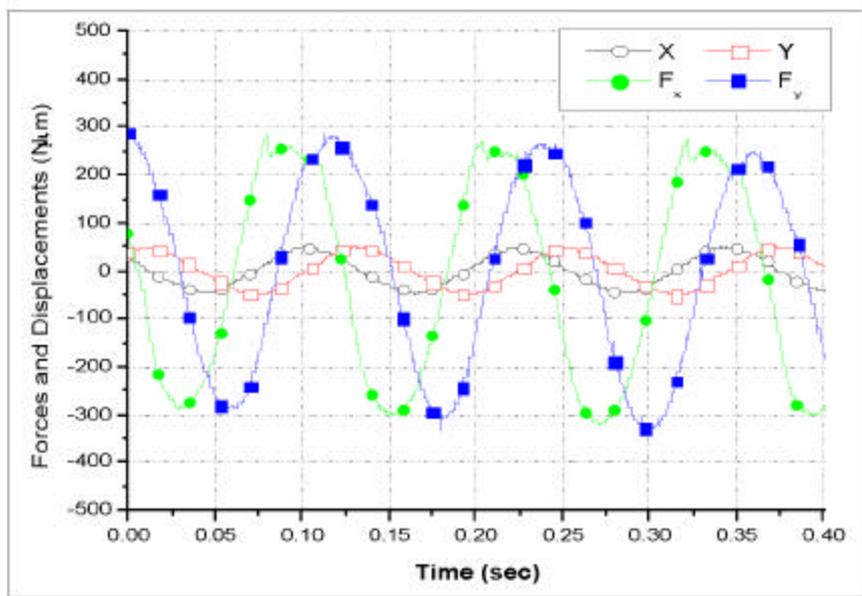


Fig.5.2 Illustration of displacements and reaction forces
(Type B, 500rpm)

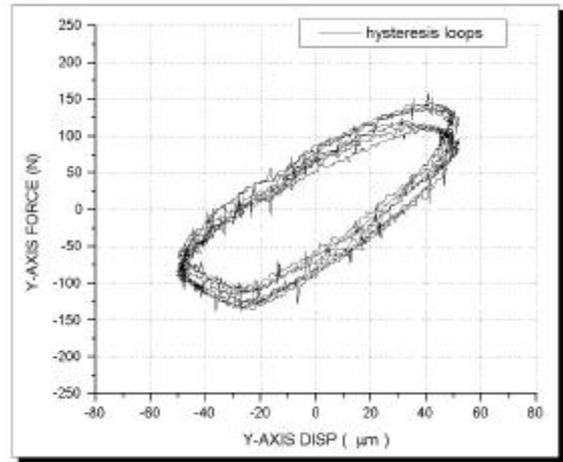
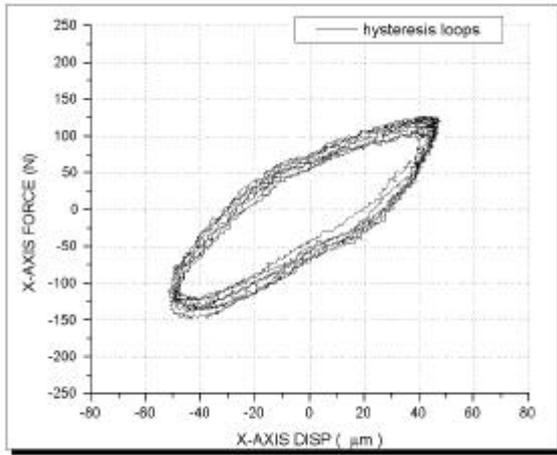


Fig.5.3 Hysteresis loops of LSD (without oil, 500rpm)

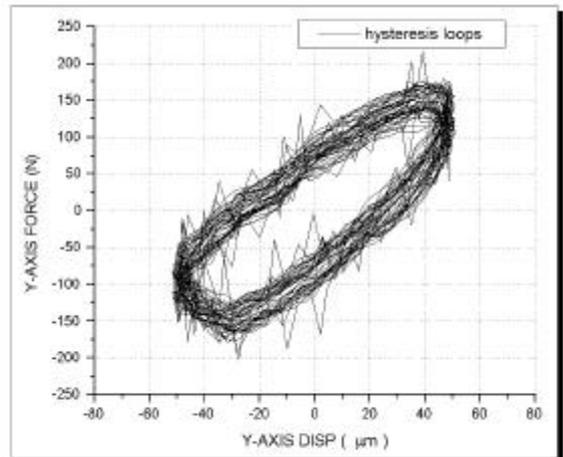
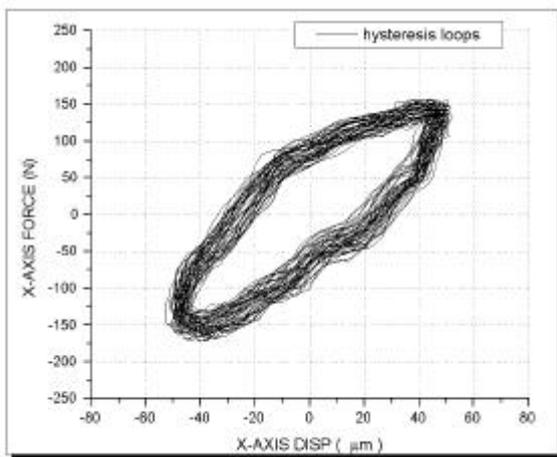


Fig.5.4 Hysteresis loops of LSD (without oil, 3000rpm)

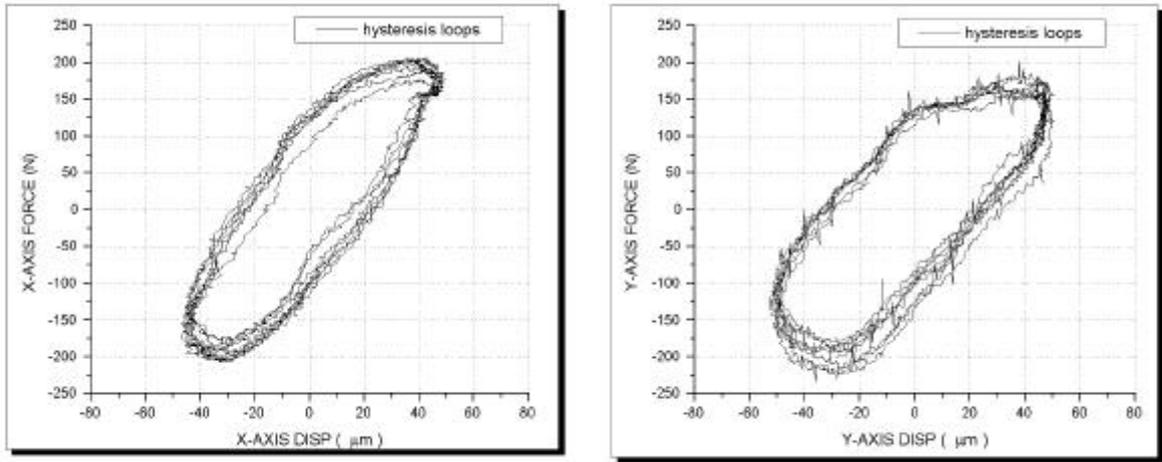


Fig.5.5 Hysteresis loops of LSD (Type A, 500rpm)

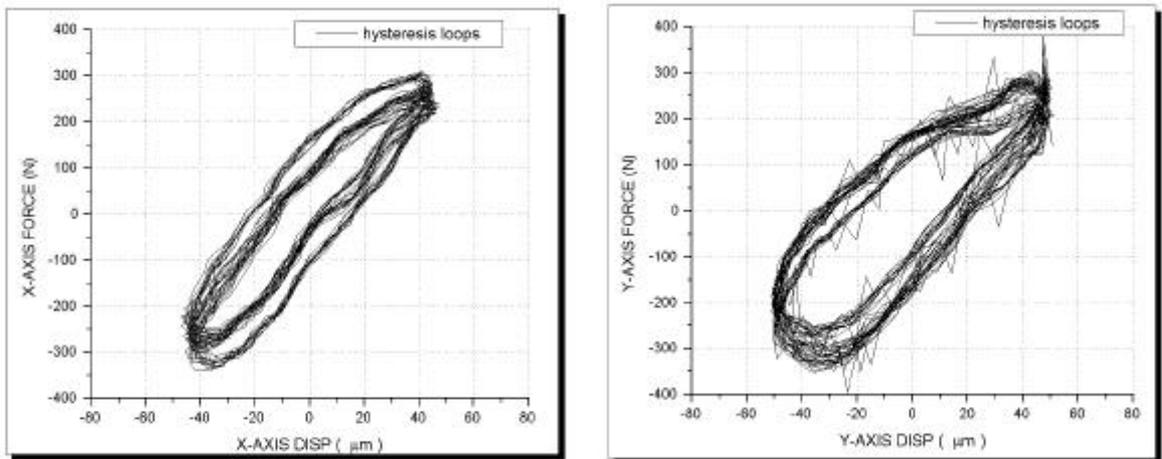


Fig.5.6 Hysteresis loops of LSD (Type A, 3000rpm)

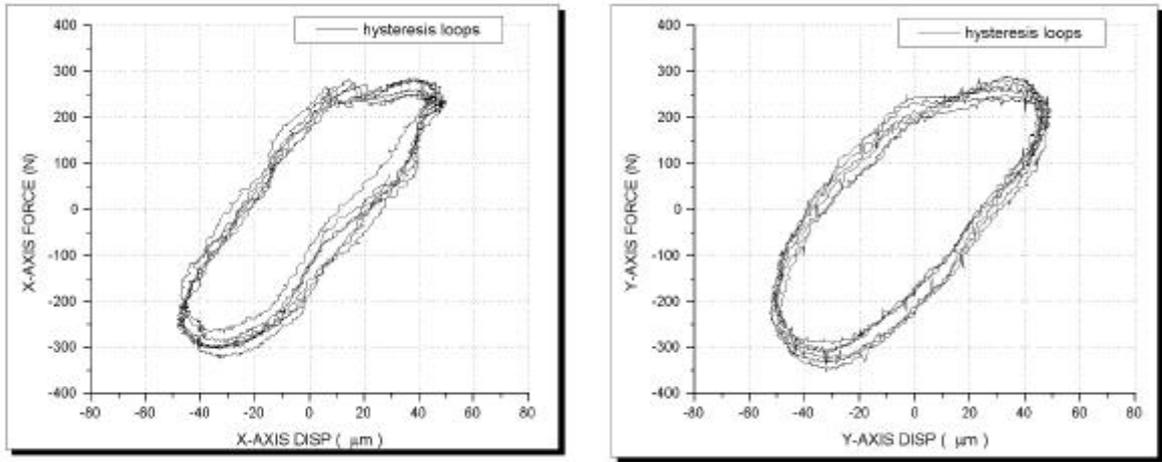


Fig.5.7 Hysteresis loops of LSD (Type B, 500rpm)

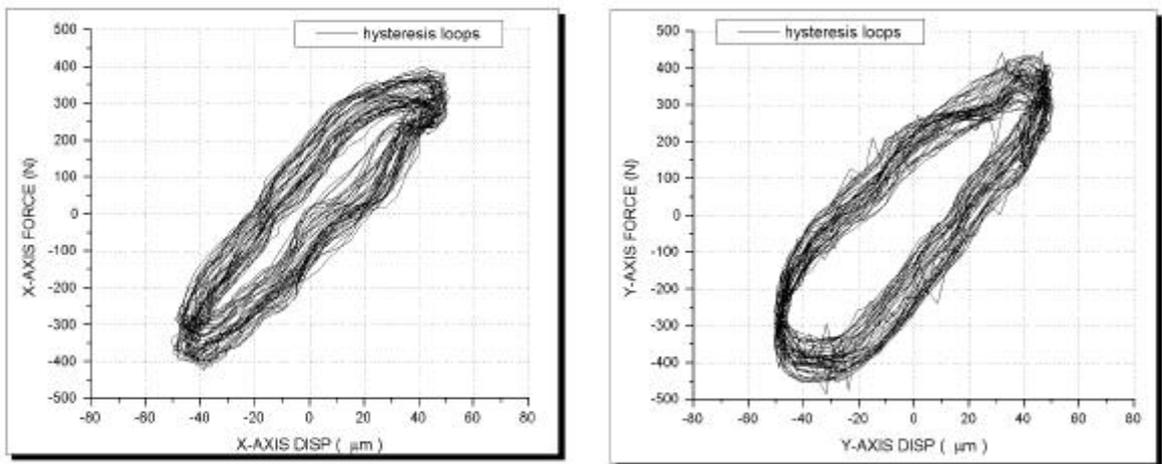


Fig.5.8 Hysteresis loops of LSD (Type B, 1000rpm)

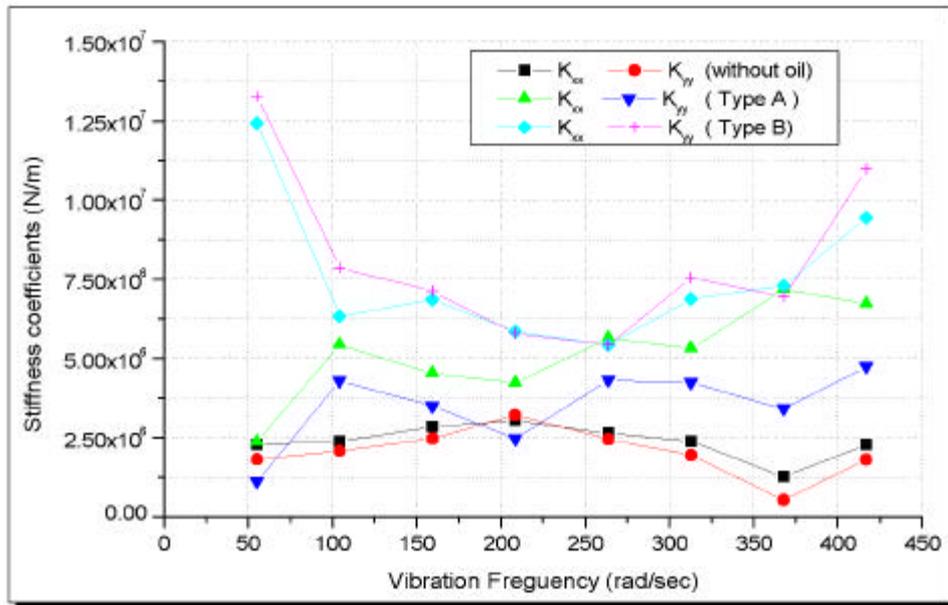


Fig.5.9 Stiffness coefficients of prototype LSD

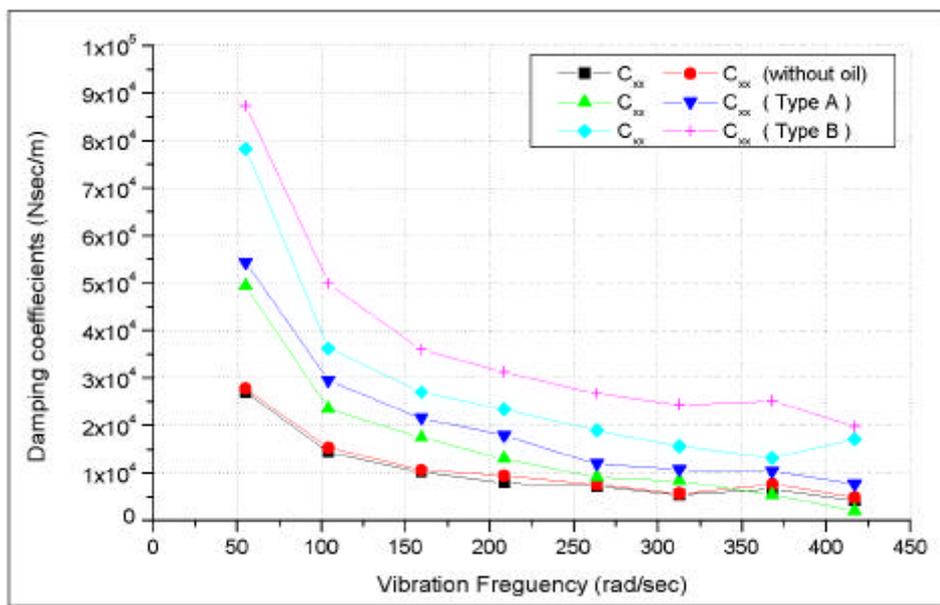


Fig.5.10 Damping coefficients of prototype LSD

LSD Hysteresis loops (X- Direction)

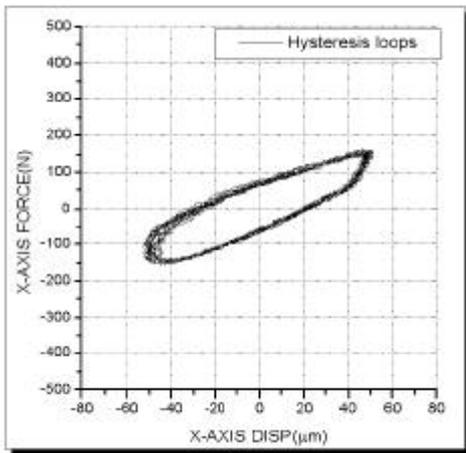


Fig.5.11 Hysteresis loops of LSD
(without oil, 1000 rpm)

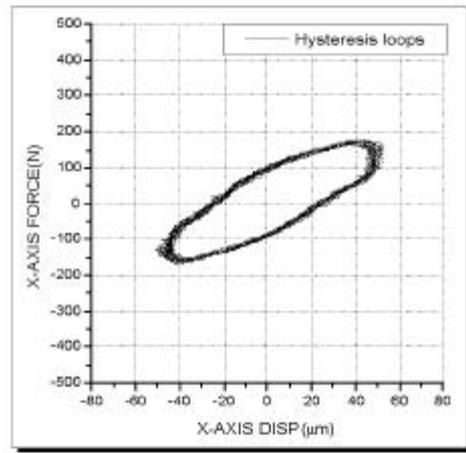


Fig.5.12 Hysteresis loops of LSD
(100 cst, 1000 rpm)

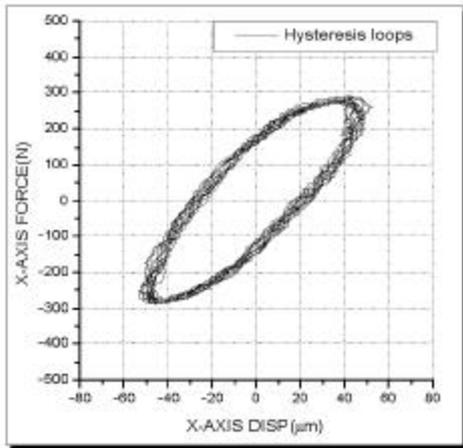


Fig.5.13 Hysteresis loops of LSD
(1000 cst, 1000 rpm)

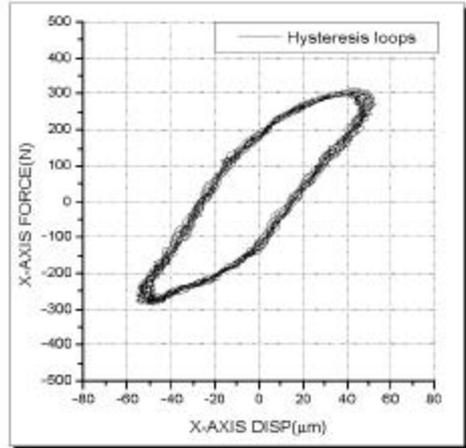


Fig.5.14 Hysteresis loops of LSD
(3000 cst, 1000 rpm)

LSD Hysteresis loops (Y- Direction)

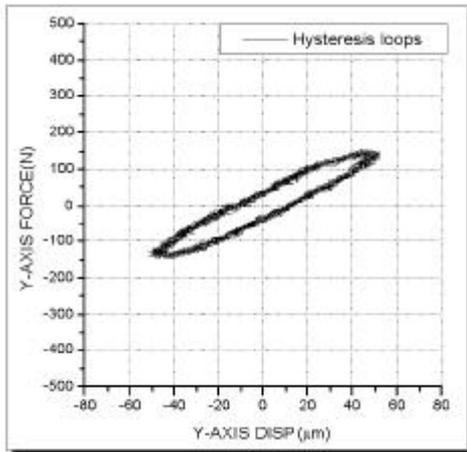


Fig.5.15 Hysteresis loops of LSD
(without oil, 1000 rpm)

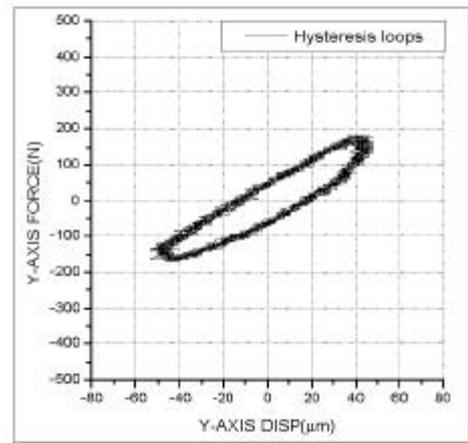


Fig.5.16 Hysteresis loops of LSD
(100 cst, 1000 rpm)

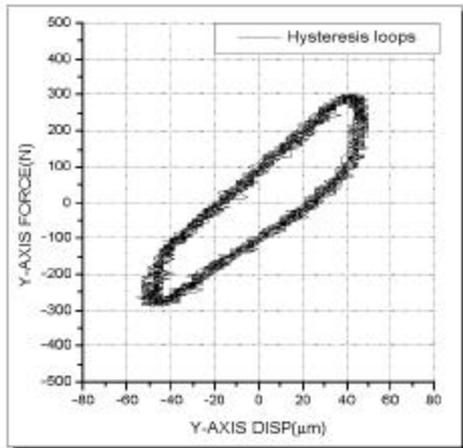


Fig.5.17 Hysteresis loops of LSD
(1000 cst, 1000 rpm)

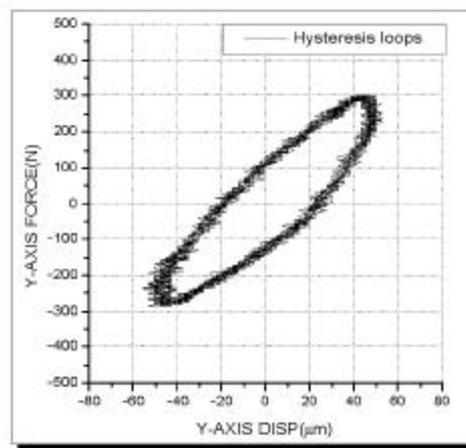


Fig.5.18 Hysteresis loops of LSD
(3000 cst, 1000 rpm)

LSD Hysteresis loops (X- Direction)

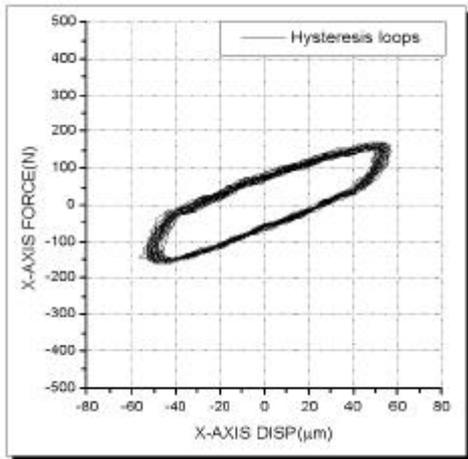


Fig.5.19 Hysteresis loops of LSD (without oil, 2000 rpm)

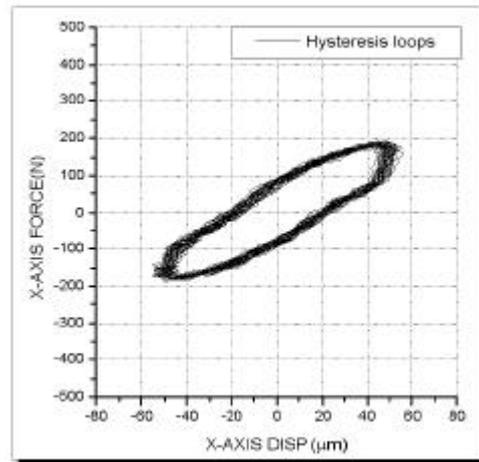


Fig.5.20 Hysteresis loops of LSD (100 cst, 2000 rpm)

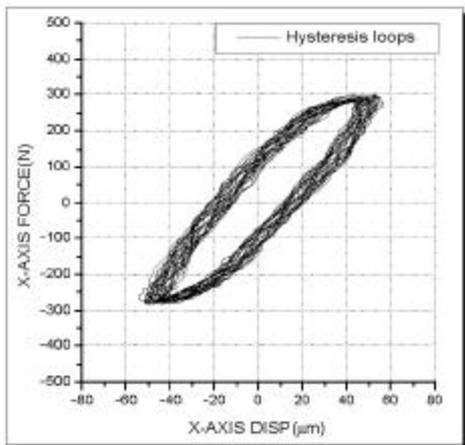


Fig.5.21 Hysteresis loops of LSD (1000 cst, 2000 rpm)

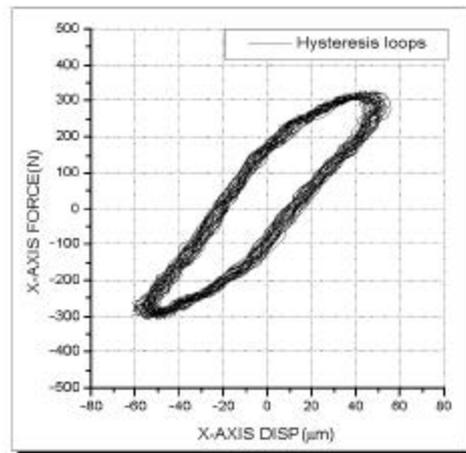


Fig.5.22 Hysteresis loops of LSD (3000 cst, 2000 rpm)

LSD Hysteresis loops (Y- Direction)

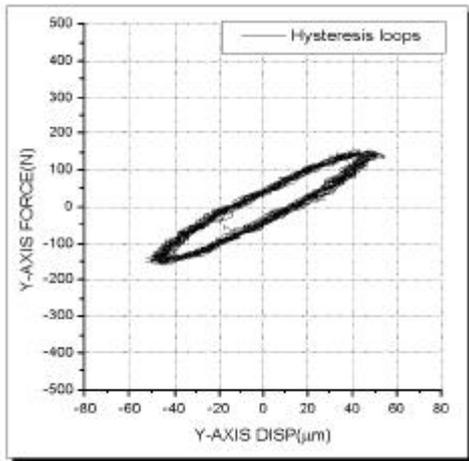


Fig.5.23 Hysteresis loops of LSD (without oil, 2000 rpm)

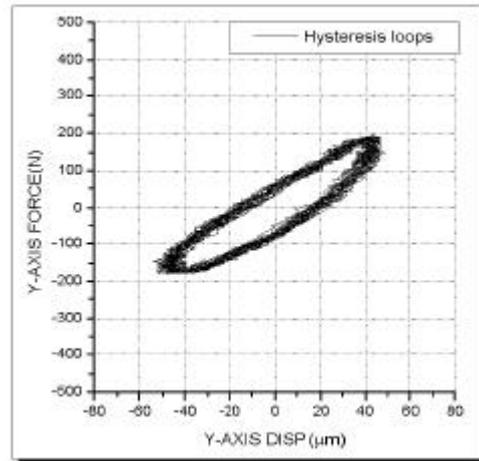


Fig.5.24 Hysteresis loops of LSD (100 cst, 2000 rpm)

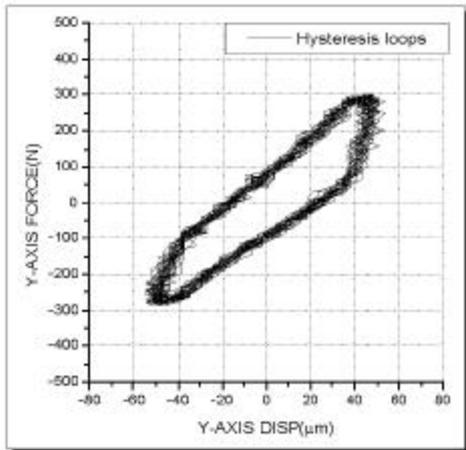


Fig.5.25 Hysteresis loops of LSD (1000 cst, 2000 rpm)

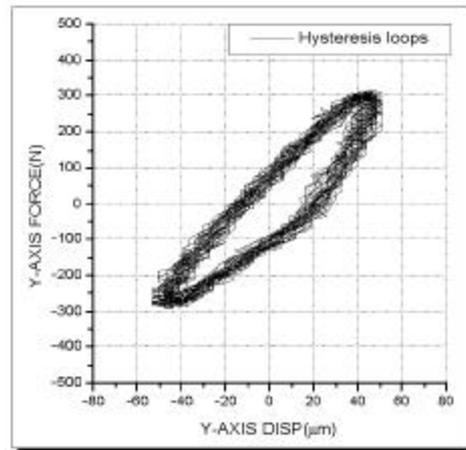


Fig.5.26 Hysteresis loops of LSD (3000 cst, 2000 rpm)

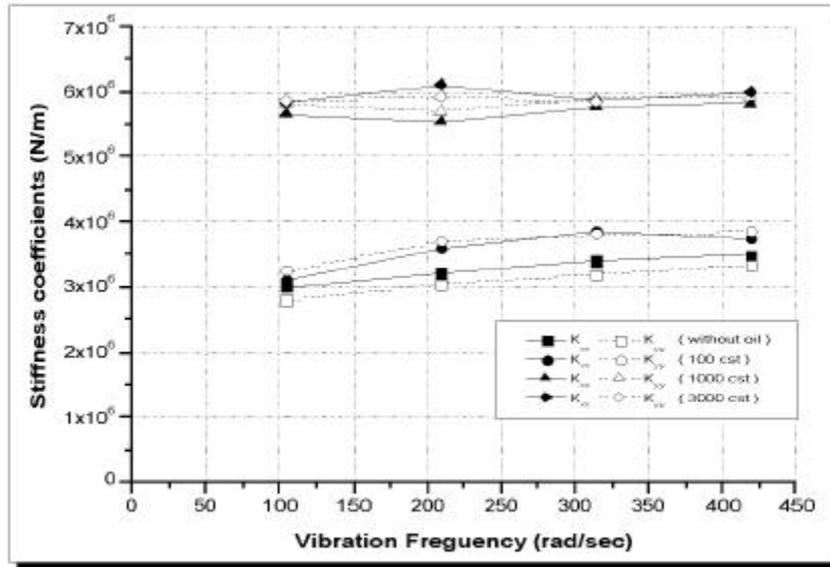


Fig.5.27 Stiffness coefficients of prototype LSD (Type C)

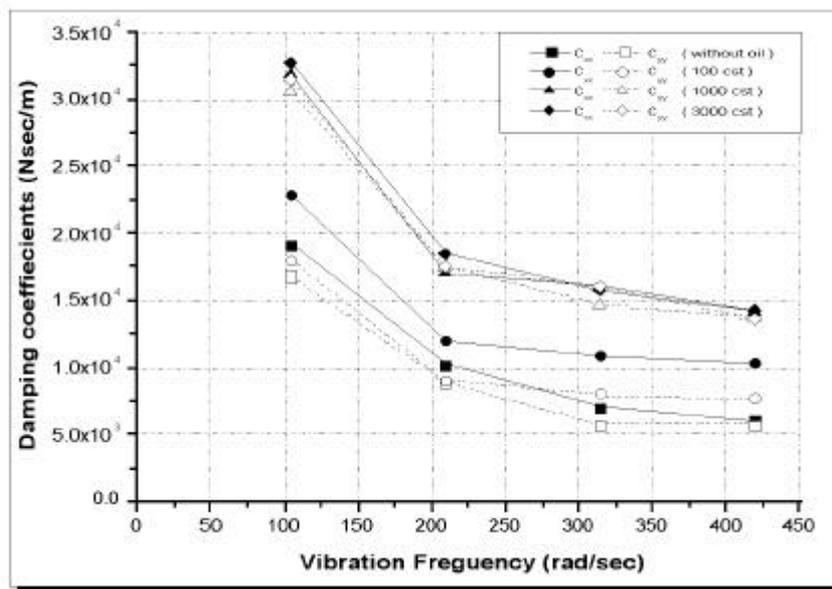


Fig.5.28 Damping coefficients of prototype LSD (Type C)

Table 4.1 Specification of prototype LSD

item	Type A	Type B	Type C	
Leaf Spring [mm]				
L1×t1	18.5 × 1.0	18.5 × 1.0	38 × 1.35	
L2×t2	18.5 × 1.0	18.5 × 1.0	34 × 1.35	
L3×t3			25 × 1.35	
width, b1	13.5	13.8	14.8	
Number of Leaf Spring pack, N	6		6	
Preload of Leaf Spring, p_e [mm]	0.1		0.25	
Oil passage[mm] width, b0	5.5		2.4	
clearance[mm], h0	0.25	0.10	0.9	
Inner ring[mm]				
inner dia, di			55.0	
outer dia, d0	92.0		71.0	
width, b	14.0		15.0	
Working oil	KF96-1000		KF96-100	KF96-3000
viscosity[cst]	1,000(@ 25 °C)		100(@ 25 °C)	3,000(@ 25 °C)
density[kg/m ³]	970(@ 25 °C)		965(@ 25 °C)	970(@ 25 °C)

Table 4.2 Specification of test rig instruments

Instrument	Specifications
<p>Gap sensor model : VS-120 maker : ono sokki co.</p>	<p>eddy current type range : 0.05 - 2.05mm linearity : 0.4% F.S</p>
<p>Gap detector model : VT-120 maker : Ono sokki co.</p>	<p>dis p, output : 0 - 5V amp. output : 0 -5V response freq. : 10Khz monitor : digital display 0 -100%</p>
<p>Load cell model : SB-200L maker : Cas co.</p>	<p>rated load : 200Kgf rated output : 2mV/V \pm0.1% excitation : 10V</p>
<p>Signal amplifier model : 2310 maker : Measurement group Inc</p>	<p>input : strain gage (50 - 1000 Ohms) output : \pm10V filter : 10Hz - 10Khz freq. response : 25Khz excitation : DC 0.5 - 15V</p>
<p>Strain amplifier model : DPM-611B maker : Kyowa electronic inst</p>	<p>input : strain gage (60 - 1000 Ohms) output : \pm5V calibration : \pm1 to \pm 99999ue filter : 10Hz - 1Khz freq. response : 5Khz excitation : AC 2V, 0.5V</p>
<p>Motor</p>	<p>power : 3.7 Kw max. rpm : 4000 rpm input : AC 180 -220 V</p>